A STATIONARY MAGNETOPLASMADYNAMIC SOURCE

V. S. Ermachenko, F. B. Yurevich,
M. N. Rolin, A. Ya. Venger,
and V. N. Borisyuk

UDC 533.95:538.4:621.384,6

A magnetoplasmadynamic source of output up to 400 kW is described, and measurements on the major electrical and thermal characteristics are reported.

It is possible to produce high enthalpy in the flowing gas with comparatively small loss in the cooled components of the discharge chamber in a system employing a ring arc in a magnetic field; this has raised considerable interest in such devices. It is usual to employ devices of comparatively low power (10-100 kW) with working flow rates not more than 0.5 g/sec [1-5]. The working gas is free from oxygen.

Devices of this type have recently been used in examining heat and mass transfer for hot gas flows [6-8]; this requires the use of higher power inputs and higher gas flow rates (G in excess of 2 g/sec), together with reasonably high enthalpy and stagnation pressure.

The magnetic field in the discharge zone in such a device has a marked effect on the energy input to the gas and also on the attainable values for the enthalpy and stagnation pressure, and it is therefore necessary to build solenoids that can produce strong fields in the steady state. This is a major difficulty in the design of a plasma accelerator of this type.

Figure 1 shows our design of source, which consists of the anode nozzle 1 and cathode 2, which are coaxial, together with the solenoid 3, which is placed with axial symmetry on the body of anode 4. The anode is made of copper and has an internal diameter of 24 mm and wall thickness 5 mm. This anode also acts as a supersonic nozzle, whose large angle (90°) facilitates the attainment of high thermal efficiency and also allows one to use highly divergent magnetic fields, which avoids leakage of the field into the space between the cathode and anode, while forcing the current to flow to the anode across the field lines, as is essential for this type of device [2].

A cooling section of appropriate shape is formed between the anode nozzle 1 and the body 4, and this carries cooling water at 25 atm. The cathode 2 is made of lanthanum-impregnated tungsten and has a length of 50 mm and a diameter of 8 mm. The tungsten cathode is mounted in the copper tube 5, which cools the cathode. This tube is insulated from the anode by the sleeve 6 made of polymethyl methacrylate. The working gas

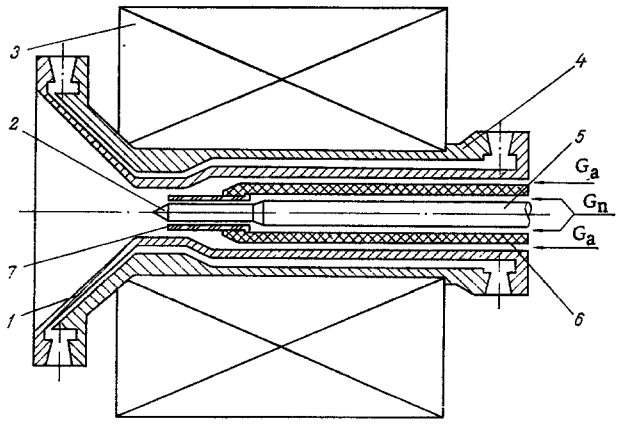

Fig. 1. Design of the magnetoplasmadynamic source.

A. V. Lykov Institute of Heat and Mass Transfer, Academy of Sciences of the Belorussian SSR, Minsk. Translated from Inzhenerno-Fizicheskii Zhurnal, Vol. 35, No. 3, pp. 459-465, September, 1978. Original article submitted March 24, 1977.

 0022-0841/78/3503-1060$07.50

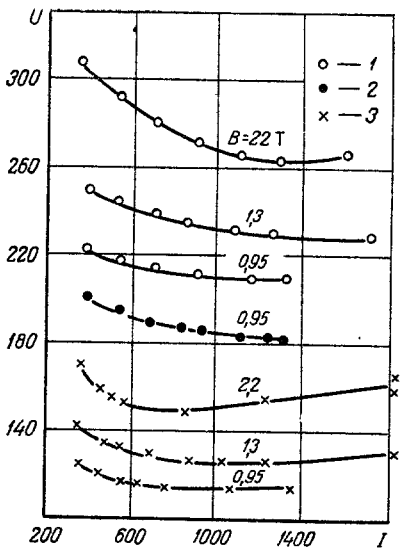

Fig. 2. Volt–ampere characteristics for the magnetoplasmadynamic source.

enters the discharge chamber via the gap between the sleeve 6 and the anode. The tungsten cathode is insulated by the fused-quartz jacket 7. There is an annular slot between the jacket 7 and the cathode that provides a means of protecting the tungsten from oxidation by impurities in the inert gas. The design of the cathode allows the latter to be moved along the axis of the accelerator.

The solenoid is wound with a square-section copper tube having a side of 5 mm and a wall thickness of 1 mm. The solenoid consists of 34 separate sections which are connected in series as regards current but in parallel as regards water cooling. The individual turns and sections are insulated with strips of glass cloth impregnated with heat-resistant lacquer. The lengths of the sections, the dimensions of the winding, and the thickness of the insulation were chosen to provide the maximum induction at the axis of the solenoid [9]. The dimensions were as follows: length 130 mm; inside and outside diameters of the windings 60 and 230 mm.

The solenoid provides an induction of 3.5 T on the axis at the center for an input of 500 kW; the maximum permissible current for a cooling-water pressure of 20 atm is 1700 A.

The power supply to the accelerator was from two mercury rectifiers of total output 2.5 MW; the maximum current was 3000 A at 825 V. Two water-cooled rheostats were used to adjust the arc and solenoid currents.

These currents were measured with a 2000-A shunt; the current and voltage were monitored continuously with N-340 chart recorders.

The heat losses in the anode and cathode were measured with differential thermocouples, which worked into an ÉPP-09 pen recorder.

The jet flowed into an evacuated chamber of volume about 3.5 m^3; this chamber was evacuated by four VN-6G pumps.

The working gas was air, while nitrogen was used to protect the cathode from oxidation. The flow rates of the two gases were controlled and monitored with reduction valves and throttles giving critical pressure differences.

The pressure in the evacuated chamber was in the range 2-11 mm Hg and was approximately proportional to the mass flow rate for G_Σ = 0.8-6.5 g/sec.

The maximum discharge input was 400 kW, which was restricted by the erosion resistance of the tungsten cathode.

The results resembled those of [4] in indicating that the working voltage was substantially dependent on the disposition of the cathode; if the cathode was displaced downstream from the zero position ($x_c = 0$), there was a fall in the voltage, but the accelerator worked unstably for $x_c \geq +10$ mm. The discharge was then no longer axially symmetrical. The voltage increased as the cathode was moved inside the anode nozzle. The accelerator worked stably up to a position where the tip of the cathode was at $x_c \geq -20$ mm; any further displacement of the cathode within the anode resulted in unstable operation.

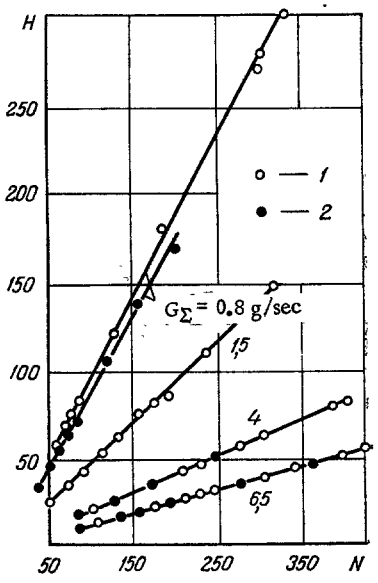

Fig. 3

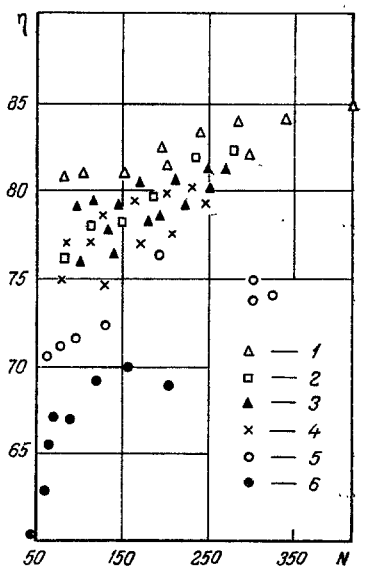

Fig. 4

Fig. 3. Mass-mean enthalpy (MJ/kg) as a function of discharge input kW: 1) B = 2.2 T; 2) 0.95.

Fig. 4. Thermal efficiency (%) as a function of discharge power (kW): 1) B = 2.2 T; G_Σ = 6.5 g/sec; 2) 0.95 and 6.5; 3) 2.2 and 4; 4) 0.95 and 4; 5) 2.2 and 0.8; 6) 0.95 and 0.8.

We found that the optimum position of the cathode for the various working conditions was $x_c = -20$ mm; this evaluation is based not only on the voltage, but also on the stability and reproducibility of the thermal characteristics.

All characteristics are subsequently given for this position of the cathode.

Figure 2 shows the volt–ampere characteristics for three gas flow rates and three values for the magnetic field at the tip of the cathode; the flow rates for the air and nitrogen were as follows: 1) $G_\Sigma = G_a + G_n = 5 + 1.5 = 6.5$ g/sec; 2) $G_\Sigma = 2.5 + 1.5 = 4$ g/sec; 3) $G_\Sigma = 0.5 + 0.3 = 0.8$ g/sec.

The shape of the volt–ampere characteristics is related to the following features of the current in the discharge in a strong magnetic field; the current flow in the plasma can be described approximately via a generalization of Ohm's law [10]:

$$\bar{j} + (\omega_e \tau_e)\left[\bar{j}\,\frac{\bar{B}}{B}\right] = \sigma_0 (E + [\bar{v}\bar{B}]). \tag{1}$$

The strong axially symmetrical magnetic field is such that $\omega_e \tau_e > 1$, and the radial conductivity of the plasma was much less than σ_0, so the field increased the resistance. The conductivity along the field remained σ_0.

The nonuniformity in the field caused some transfer of the current to the region of lower B.

The accelerating force acting on unit volume of plasma is due to intersection between the current and the field lines and is $[\bar{j}\bar{B}]$.

An induction effect arises when the field lines intersect the plasma, which corresponds to the $[\bar{v}\bar{B}]$ in (1).

The plasma conductivity is of tensor character, so there are currents in the radial, azimuthal, and axial directions; the interaction between the magnetic field and these currents sets up forces in the corresponding directions. The radial component of the force is directed along the axis.

The volt–ampere characteristics are of falling type at low currents on account of the rapid increase in the conductivity as the plasma temperature rises, which results from a rapid increase in the free-electron concentration. The electron mobility tends to fall at high temperatures or when the ion concentration reaches

a certain level on account of the increase in the frequency of collisions between the ions and electrons, which retards the increase in the conductivity, in spite of the increase in the electron concentration. Consequently, the voltage–ampere characteristic becomes of rising type.

The values for the Hall factor $\omega_e\tau_e$ may be extremely large at low degrees of ionization; this results in very considerable displacement of the current. However, this quantity falls rapidly as the temperature rises on account of the increase in the collisional frequency, and this reduces the current displacement. When the region of complete ionization is approached, the fall in $\omega_e\tau_e$ tends to become rather less, and ultimately $\omega_e\tau_e$ begins to rise, which is due to the reduction in the collisional cross sections at high temperatures.

The shape of the volt–ampere characteristics is only slightly affected by the inherent field set up by the arc current in the range of arc currents and gas flow rates used.

The $\omega_e\tau_e$ parameter increases with the field strength, which causes the voltage to rise.

The radial conductivity varies roughly in inverse proportion to the square of $\omega_e\tau_e$; however, the increase in the current displacement accompanies increases in the pressure and temperature in the discharge zone to cause the voltage to increase linearly. A similar result has been reported previously [2, 4, 7].

The slopes of the two branches in the volt–ampere characteristic increase with the field strength for a given flow rate because the enthalpy is more dependent on the current at high fields (high voltages). The minimum on the volt–ampere characteristic shifts to the left as the field strength increases. The voltage minima correspond to enthalpies of about 100 and 50 MJ/kg for working flow rates of 0.8 and 6.5 g/sec, respectively.

The voltage increases and the slope of the volt–ampere characteristic decreases as the working-gas flow rate is raised.

Figure 3 shows the enthalpy as a function of discharge power for various field strengths and flow rates; the enthalpy increases considerably as the flow rate is reduced or the power input is increased. Fields in the range 0.95-2.2 T have virtually no effect on the enthalpy at high flow rates (G_Σ = 4 and 6.5 g/sec), which is due to the very slight dependence of the efficiency on the induction in that range for a given input power. There is a slight increase in the enthalpy with the field for G_Σ = 0.8 g/sec, which is due to an appreciable increase in the efficiency as the field increase from 0.95 to 2.2 T.

Figure 4 shows the thermal efficiency as a function of input power for two field strengths and three flow rates; there is an appreciable increase in the efficiency with flow rate.

The loss in the anode was approximately proportional to the arc current and was almost independent of the flow rate and magnetic field; this indicates that the loss is largely due to the potential drop in the region near the anode [2].

The behavior of the thermal efficiency is in accordance with

$$\eta = 1 - \frac{\Delta v_a}{U(G_\Sigma, B, I)},$$

where Δv_a is a coefficient of proportionality, which itself is related to the thermal loss associated with the arc current.

The result from processing the experimental data was Δv_a = 40 V.

Major parameters related to the aerodynamic heating are the heat flux and the stagnation pressure; these were estimated for various working conditions and various distances from the end of the anode nozzle.

The heat flux was measured with transducers of calorimetric type; we used stationary devices (water cooled) and nonstationary ones (regular mode). The diameter of the flat end of a detector was 20 mm.

The stagnation pressure was measured with a total-pressure device; stagnation pressures up to 0.05 atm were obtained with our working conditions, which corresponded to plasma jets representing heat fluxes at the cold wall of the calorimeter in the range 0.05-4 kW/cm^2.

We found that an erosion-resistant cathode capable of working at currents above 2000 A allowed us to increase the input power at the maximum attainable magnetic field strength in the discharge zone. This made it possible to produce air-plasma jets having a mass-mean enthalpy H > 300 MJ/kg.

NOTATION

I is the current;
U is the voltage;
N is the discharge power;
B is the induction;
H is the enthalpy;
η is the thermal efficiency;
x_c is the distance between the cathode and end of anode cone;
j is the current density;
E is the electric field;
v is the plasma speed;
e is the electron charge;
m_e is the electron mass;
τ_e is the mean time between electron collisions;
$\omega_e = eB/m_e$ is the cyclotron frequency;
$\omega_e\tau_e$ is the Hall parameter;
σ_0 is the plasma conductivity in absence of magnetic field.

LITERATURE CITED

1. W. Grossman, R. V. Hess, and H. A. Hassan, AIAA J., No. 6 (1966).
2. R. M. Patrick and A. M. Schneiderman, AIAA J., No. 2 (1966).
3. P. Brockman, R. Hess, F. Bowen, and O. Jarret, AIAA J., No. 7 (1966).
4. A. M. Schneiderman and R. M. Patrick, AIAA J., No. 10 (1966).
5. G. A. Luk'yanov and V. V. Sakhin, Zh. Prikl. Mekh. Tekh. Fiz., No. 6 (1975).
6. G. W. Garrison and R. T. Smith, AIAA J., No. 9 (1970).
7. E. R. Pugh, R. M. Patrick, and A. M. Schneiderman, AIAA J., No. 2 (1971).
8. Academician L. A. Artsimovich (editor), Plasma Accelerators, [in Russian], Mashinostroenie, Moscow (1972).
9. D. B. Montgomery, Solenoid Magnet Design, Wiley (1969).
10. D. A. Frank-Kamenetskii, Lectures on Plasma Physics [in Russian], Atomizdat, Moscow (1968).